Quantum Monte Carlo and Electron Localization Function Study of the Electronic Structure of CO_2^+

A. C. Kollias and W. A. Lester, Jr.

Chemical Sciences Division, Lawrence Berkeley National Laboratory and

Kenneth S. Pitzer Center for Theoretical Chemistry, Department of Chemistry,

University of California, Berkeley, CA 94720-1460

ABSTRACT: The atomization energy and heat of formation of CO_2^+ are computed using the diffusion Monte Carlo (DMC) variant of quantum Monte Carlo (QMC) and compared with values determined at the Moller-Plesset second order (MP2), a generalized gradient approximation density functional theory (B3LYP-DFT), the coupled-cluster singles-doubles with perturbative triples [CCSD(T)] levels of theory. Hartree-Fock (HF) and complete active space self-consistent field (CASSCF) trial functions were used in the DMC calculations. A CASSCF trial function (TF) was found to yield an 8.1 kcal/mol improvement for both properties relative to the HF TF value. The DMC calculation with the HF TF gave an atomization energy of 374.0 kcal/mol, while the DMC result with the CASSCF TF yielded 382.1 kcal/mol; the experimental atomization energy is 381 kcal/mol. The DMC heat of formation is: 234.7 kcal/mol using the HF TF and 226.7 kcal/mol using the CASSCF TF. These values lie closer to experiment than results obtained from the MP2, DFT, and CCSD(T) methods, all at the complete basis set limit.

The bonding character of CO_2^+ and CS_2^+ was examined using the electron localization function (ELF) method. The HF, MP2, and B3LYP-DFT wave functions were projected onto the single-triple and double-double resonance forms of the molecules to determine the relative contribution of the two forms to the ground state geometry. The

double-double resonance form was found to be the larger contributor to the ground state for both systems.

KEYWORDS: Quantum Monte Carlo, CO_2^+ heat of formation, CS_2^+, electron localization function, quantum-chemical calculations

Introduction

The CO_2^+ molecule presents difficulties for the calculation of various properties, even though the system has the well-defined $D_{\infty h}$ symmetry experimentally in the electronic ground state [1, 2]. Moller-Plesset second order (MP2) and higher orders of MP perturbation theory generate symmetry breaking, reducing the symmetry to $C_{\infty v}$ until one reaches the MP5 level [3, 4]. The C-O bond length has previously been accurately computed using several other levels of theory. In particular B3LYP-DFT[4], a generalized gradient approximation density functional theory method, recovers the experimentally observed distance. It is also noted that methods that only include single and double substitutions from a single determinant starting point such as MP2, configuration interaction singles (CIS) and CI singles and doubles (CISD) give an incorrect description of the asymmetric stretching frequency ω_3 [4]. Methods that include triple and higher substitutions yield improved values of this quantity

Problems in accurately computing the geometry of CO_2^+ are postulated to arise because of competition between two resonant forms of the molecule: a single-triple (S-T) and a double-double (D-D) bonded structures [5] (Fig. 1). Overemphasis of the D-D structure results in asymmetric stretching frequencies that are high compared to experiment, while overemphasis of the S-T structure leads to low asymmetric stretching frequencies and symmetry breaking. Earlier studies using a variety of methods have noted that triple excitations are required to give the correct geometry as well as accurate description of the normal modes of the system [4].

Quantum Monte Carlo (QMC), a method that exactly solves the Schrödinger equation through stochastic sampling of a trial wave function, has been found successful in treating the ground states of systems that have posed problems for other electronic structure methods. Considering the difficulties that have been encountered with CO_2^+ using other approaches such as MP2, CIS, and CISD, we chose to examine this system with QMC in the more accurate diffusion Monte Carlo (DMC) form of the method. We have computed the atomization energy and heat of formation using DMC and compare these results with those generated with the restricted open shell Hartree-Fock (ROHF), MP2, local density approximation (LDA), B3LYP-DFT, and coupled-cluster with single and double excitations with inclusion of triple excitation by perturbation theory (CCSD(T)) methods.

To our knowledge a study to determine and quantify the contribution of the resonance structures to the ground state geometry and frequency of CO_2^+ has not been carried out. We have determined the bonding character of this system at the experimental (symmetric) C-O bond length of 1.177A [1, 2, 4] and two asymmetric geometries using the electron localization function (ELF) to determine the contributions of the resonance forms to the ground state geometry. The ELF findings also shed light on the contribution of resonance forms to the asymmetric stretching frequency at several levels of theory.

While symmetry breaking is encountered in the MP2 CO_2^+ calculations, similar calculations of isovalent CS_2^+ do not reveal symmetry breaking even though the ground

and first-excited states are more closely spaced (20,975 cm^{-1}) than in CO_2^+ (27,300 cm^{-1}) [2, 6]. Because of the closer spacing in CS_2^+, it might be expected that vibronic state mixing could play a role leading to dominance in the ground state of the S-T configuration. With the ELF method, we show that charge localization is more important than the separation of the states in determining the dominant resonance structure for the ground state geometry.

The remainder of the paper is organized as follows: Sec. II contains a brief summary of DMC, highlighting the basic ideas and concepts of the method; and Sec. III presents the DMC and other ab initio computations of the atomization energy and heat of formation of CO_2^+. Section. IV summarizes the main aspects of ELF methods and in Sec. V, the results of ELF projections are presented and discussed. Conclusions of the study form the content of the last section.

II. The DMC Method

The DMC method is a stochastic approach for solving the Schrödinger equation in imaginary time τ. The latter can be written,

$$\frac{\partial \phi}{\partial \tau} = D\nabla^2 \phi(x,\tau) + (E_T - V(x))\phi(x,\tau) \qquad (1)$$

where E_L is an energy offset, D is a diffusion constant, $D \equiv 1/2m$, and $V(x)$ is the potential. Note that retaining only the first term on the rhs of Eq.(1) defines a diffusion equation if φ is positive definite; retaining only the second term on the rhs yields an equation that describes branching or population growth/decay. The asymptotic solution of

Eq.(1) is the time-independent Schrödinger equation. Because the potential $V(x)$ can vary over the range $\pm\infty$, the branching term typically leads to large statistical uncertainty in the energy expectation value. These fluctuations can be reduced significantly by importance sampling.

The analog of Eq.(1) with importance sampling is obtained by multiplying both sides of Eq.(1) by a known function Ψ_T. One defines a new function given by :

$$\mathrm{f}(\mathrm{x},\tau) = \Psi_{\mathrm{T}}\Phi(x,\tau) \tag{2}$$

where $\Phi(x,\tau)$ is an exact solution to the Schrödinger equation. Following this procedure, Eq. (1)takes the form [7]

$$\frac{\partial f(x,\tau)}{\partial \tau} = D\nabla^2 f(x,\tau) - D\nabla(f(x,\tau)F_Q(x)) + (E_T - E_L(x))f(x,\tau) \tag{3}$$

where E_L is the local energy defined as

$$E_L \equiv \frac{\hat{H}\Psi_\tau(\vec{X})}{\Psi_\tau} \tag{4}$$

$\vec{X}$ denotes the $3N$ coordinates of the system, and $F_Q(\vec{X})$ is a vector field labeled the quantum force given by

$$F_Q \equiv \nabla \ln\left|\Psi_\tau(\vec{X})\right|^2 \tag{5}$$

The quantum force moves the walkers from regions of high to low potential, which reduces the magnitude of random fluctuations and helps stabilize the walker population. To insure a positive definite distribution f, the fixed node approximation is made which imposes the known nodes of Ψ_T onto Φ .

The trial wave function Ψ_T is chosen as a product of an independent-particle function ψ, and an explicit correlation function $U\left(\{r_{ij}\},\{r_{i\alpha}\},\{r_{i\beta}\}\right)$ where r_{ij} is the

distance between electrons i and j, and $r_{i\alpha(\beta)}$ is the separation of electron i from nucleus $\alpha(\beta)$. The form of U used here is a 10-parameter function adapted by Schmidt and Moskowitz [8] from earlier work of Boys and Handy [9] (SMBH). This function contains both 2- and 3-body terms in the form of electron-electron, electron-nucleus, and electron-other-nucleus distances and may be written,

$$U \equiv \sum_{k}^{N_a} c_{ka} (\vec{r}_{ai}^{\,l_{ka}} \vec{r}_{aj}^{\,m_{ka}} + \vec{r}_{aj}^{\,l_{ka}} \vec{r}_{ai}^{\,m_{ka}}) \vec{r}_{ij}^{\,n_{ka}} \tag{6}$$

where α refers to nuclei and ij refer to electrons and where $\vec{r}$ is defined by $\vec{r} = 1/(1+br)$ and b is a variational parameter. The SMBH correlation function contains first-order Jastrow terms that assist in satisfying electron-electron and electron-nuclear cusp conditions [10, 11]. Optimization of the correlation functions parameters was accomplished by fixed sample optimization using the absolute deviation functional [12] (AD) that minimizes the variance and energy of Ψ_T

$$AD \equiv \frac{1}{N} \sum_{i=1}^{N} \left| E_T - E_{L_i} \right| \tag{7}$$

Here N is the number of walkers in the simulations and E_L is the local energy of the i^{th} configuration. The trial wave function Ψ_T is typically written in the form,

$$\Psi_\tau \equiv D^{\uparrow} D^{\downarrow} \exp\left(U(r_{ij}, r_{i\alpha})\right) \tag{8}$$

where $D^{\uparrow} D^{\downarrow}$ denote spin block-factored determinants. The nodes of the independent particle function are the zeros of a HF trial wave function of molecular orbitals (MOs) or of natural orbitals from a complete active space self-consistent field (CASSCF) calculation.

The Stevens, Basch, and Krauss (SBK) pseudopotentials[13, 14] were used in the construction of the DMC trial wave functions reported here in order to reduce the computational effort. The other ab initio calculations used the cc-pVXZ (X=D,T,Q) basis set series [15]. This series of basis sets is frequently used in complete basis set extrapolations, which were also carried out in this study. The cc-pVTZ basis was used in conjunction with the SBK pseudopotentials.

III DMC and other ab initio results

Two trial wave functions were used in the DMC computations performed in this study. The first trial function used HF orbitals and the other used the NOs obtained from a CASSCF(7,8) calculation. The CASSCF calculation yielded 17 determinants of which the first determinant recovered 95% of the ground state energy of CO_2^+. Examining the NO population at the MP2 level of theory revealed an incorrect NO population description. In two of the orbitals the orbital population was greater than 2 and in three orbitals the orbital population was negative, implying that the MP2 method improperly describes the ground state populations of the NOs. The orbital populations obtained from the CASSCF(7,8) revealed that all orbital populations are between 0 and 2 [16]. These results are presented below in Table 1. The NO's obtained from this CASSCF give a more accurate, atomization energy and heat of formation than the MO's obtained from HF.

The geometry of CO_2^+ used in this study was obtained using a generalized gradient approximation B3LYP-DFT method [17] with the cc-pVDZ basis set. The resulting $C-O$

bond lengths of 1.17741A are in excellent agreement with experimental. Geometry optimization with the MP2 method, resulted in symmetry breaking of the $C-O$ bond length observed in earlier studies. The LDA and CCSD(T) $C-O$ bond lengths of 1.188 A are in good agreement with experiment though not as accurate the B3LYP-DFT.

For the DMC calculations the Gaussian basis sets were mapped onto a polynomial basis of cubic splines. For each nuclear center 2000 evenly spaced spline knots were used. The use of splines makes possible more efficient Slater determinant evaluation as confirmed by the reduction of computational effort of 45%-55% relative to the use of Gaussian basis functions.

The atomization energy, E_a, defined as the energy required to dissociate a molecule into its atomic constituents was computed to be 381 kcal/mol CO_2^+ using the expression:

$$E_a\left(CO_2^+\right) = 2\Delta H_f(O) + I_P(O) + \Delta H_f(C) - \Delta H_f(CO_2) - I_P(CO_2) \tag{9}$$

The QMC estimate of E_a using effective core potentials without zero point energy correction is determined as the difference in valence energy of the constituent atoms and the molecular system and is given by,

$$E_a\left(DMC\right) = E_{DMC}\left(O\right) + E_{DMC}\left(O^+\right) + E_{DMC}\left(C\right) - E_{DMC}\left(CO_2^+\right) \tag{10}$$

To estimate the heat of formation, ΔH_f^{298} of the cation the following expression was used[18]

$$\Delta H_f^{298}(DMC) = \Delta H_f^0(C) + 2\Delta H_f^0(O) + I_P(O) + ZPE_{co_2^+} - \left[Temp + E_a(DMC)\right] \tag{11}$$

where $Temp$ is the gas-phase temperature correction from 0 to 298 K and $ZPE_{CO_2^+}$ is the zero point energy. Values for Eqs. (9) and (11) were obtained from standard thermochemical tables [19],[20]. The experimental zero point energy was used at all levels of theory for the ΔH_f^{298} estimates. The ZPE value was obtained using:

$$ZPE \equiv \frac{1}{2} hc \sum_{i=1}^{3N-6} \nu_i \tag{12}$$

where ν_i are the fundamental frequencies [6].

The atomization energy and heat of formation were calculated using the cc-pVXZ (X=D,T,Q) series of basis sets. Complete basis set extrapolations were determined using an exponential fit. Results of the ROHF, MP2, LDA, B3LYP, CCSD(T) and DMC calculations of the atomization energy and heat of formation are presented in Table 2. The results of the MP2 calculations overestimate the atomization energy by 15.1 kcal/mol while the heat of formation is underestimated by 15 kcal/mol; LDA calculations gave similar results. LDA overestimates the atomization energy by ~19% and underestimates the heat of formation. The B3LYP estimates of the atomization energy with an infinite basis are 1.7 kcal/mol below the experimental value and the heat of formation is 4.2 kcal/mol above the experimental value. At the complete basis set limit, the CCSD(T) atomization energy is 0.7 kcal/mol below experiment and the heat of formation is 3 kcal/mol above experiment.

The DMC method with the HF MOs yields an atomization energy that is 7 kcal/mol less than experiment while the heat of formation estimate is 9 kcal/mole above experiment. The DMC method with CASSCF NOs in a single determinant leads to closer agreement with experiment for both the atomization energy and heat of formation by 8.1 kcal/mole. The DMC and experimental heats of formation are 226(1.8) kcal/mol and 225.3 kcal/mol, respectively; the DMC and experimental atomization energies are 382(1.8) kcal/mol and 381 kcal/mol, respectively.

IV Electron Localization Function (ELF)

In this study we have used an approach based on the electron localization function (ELF) method developed by Becke and Edgecombe to analyze the bond character of CO_2^+ [21]. The approach provides a picture of the molecule structure and reactivity by considering bonds and their evolution [22, 23]. The ELF has an associated topology that is partitioned into specific regions. Molecular space is partitioned into basins: core basins around the nuclei and valence basins in the remaining space. Properties such as basin populations, basin volumes and basin populations' variance are evaluated with ELF. Previous studies have demonstrated that the partitioning of the molecular space is qualitatively stable under changes arising from the use of various theoretical methods to specify the ELF [22, 24, 25]

The electron localization function is a measure of the excess kinetic energy of in the system, essentially quantifying the efficiency of Pauli repulsion at a given point. The ELF is defined as

$$ELF \equiv \frac{1}{1+\chi_\sigma^2} \tag{13}$$

where χ_σ is a dimensionless localization index calibrated to the uniform electron gas as a reference, written as:

$$\chi_\sigma = \frac{D_\sigma}{D_\sigma^0} \tag{14}$$

where D_σ^0 is the uniform electron gas spin density evaluated at $\rho_\sigma(r)$, the one-electron spin density and given by

$$D_\sigma^0 = \frac{3}{5}\left(36\pi^4\right)^{\frac{1}{3}} \rho_\sigma^{\frac{5}{3}}(r) \tag{15}$$

The term D_σ is the first term of the spherically averaged Taylor expansion of a pair probability:

$$D_\sigma = \tau_\sigma - \frac{\left(\nabla\rho_\sigma\right)^2}{4\rho_\sigma} \tag{16}$$

The quantity, D_σ, gives an inverse relationship between localization; the higher the degree of localization the smaller the value of D_σ. For this reason Eq. (16) is arbitrarily recast to the final ELF given in Eq. (13). The bounds on the value of ELF are:

$$0 \le ELF \le 1 \tag{17}$$

where $ELF = 1$ corresponds to perfect localization and $ELF = \frac{1}{2}$ corresponds to electron gas pair probability. Quantitative information similar to population analysis can be obtained from the partitioning scheme. The average basin population which only depends on the single particle density, is defined as

$$\bar{N}_i(\Omega_i) = \int_{\Omega_i} \rho(r)dr \tag{18}$$

where Ω_i is the volume of the ith basin

.

The Lewis representation of a system can be obtained by projecting the ELF populations, $N(\Omega_i)$, onto one or more Lewis structures. Given two or more resonance structures the ELF populations can determine the weight of each resonance structure to the total Lewis description of the system, in essence a quantization of the Lewis resonance forms. The present ELF calculations were carried out using the TopMoD [26] package. Wave functions for the ELF calculations were obtained using Gaussian 98 [27] and GAMESS [28] software packages.

V. Topological Analysis:

Previous studies have examined the dipole moment and bond order of CO_2^+ as a function of the asymmetric stretch [4]. In this study basin population analysis of unrestricted Hartree-Fock (UHF), MP2, and B3LYP-DFT wave functions was carried out by projecting these populations onto resonance forms of CO_2^+ and CS_2^+. The wave functions were projected onto the ground state geometry from two perturbed geometries that consisted on stretching one of the $C-X$ $(X=O,S)$ bond lengths from the equilibrium distance by 0.005 A and 0.01 A. From these projections it is possible to quantify the relative contributions of the $S-T$ and $D-D$ configurations in the ground state geometry. The topologies obtained for both structures are qualitatively the same at all levels of theory, having the same number of core and valence regions. Figure 1 presents the ELF valence and core regions for CO_2^+

CO_2^+ Analysis

An ELF analysis reveals that there are 9 basins of attraction in the system: 3 core basins $C(C), C(O_1)$ and $C(O_2)$, two valence basins located between the carbon and oxygen atoms, $V(C,O_1)$ and $V(C,O_2)$ two valence basins located on each of the oxygen atoms: $V(O_1)$ and $V(O_2)$. The projections of the basin populations for UHF, MP2, and B3LYP wave functions with the cc-pVDZ and cc-pVTZ basis sets were computed at the experimental geometry, and at small deformations of 0.005 A and 0.01 A along one of the $C-O$ bonds.

The relative contributions the $S-T$ and $D-D$ structures can be determined by projecting the populations of the basins onto the resonance structures by examining the number of electrons (core and valence) on each oxygen atom in the two configurations. The following linear system can be written for the number of electrons surrounding an oxygen atom:

$$9w_1 + 10w_2 = \alpha \tag{19}$$

$$10w_1 + 9w_2 = \gamma \tag{20}$$

where α and γ are the sum of valence and core basins of O_1 and O_2.

$$\alpha = 2V(C,O_1) + C(O_1) + 2V(O_1) \tag{21}$$

$$\gamma = 2V(C,O_2) + C(O_2) + 2V(O_2) \tag{22}$$

The coefficients of Eqs. (21) and (22) are the number of electrons surrounding O_1 and O_2. Solving Eqs (21) and (22) for w_1 and w_2 for the UHF, MP2, and B3LYP-DFT methods gives the contributions of the resonance forms for the respective methods. To avoid overestimation of the local topological descriptions, the normalization condition, $w_1 + w_2 = 1$, has not been imposed. Any deviation from the normalization condition of the sum of the solutions can be interpreted as the contribution of an unknown structure (X) or attributed to numerical error of the integration method. The contribution results for UHF, MP2, and B3LYP-DFT wave functions for both cc-pVDZ and cc-pVTZ basis sets are given in Table 3.

The results of the population projections of the UHF wave function for the cc-pVDZ and cc-pVTZ basis sets, indicate a small preference for the $S-T$ configuration at the experimental geometry. Small deformations of 0.005 A and 0.01 A of one of the $C-O$ bonds, for the cc-pVTZ and cc-pVDZ basis sets, leads to increased emphasis of the $S-T$ configuration.

Examining the MP2 results of the basin population projections shows results similar to those found with the UHF wave function. At the experimental $C-O$ 1.177 . bond length the $S-T$ structure is slightly preferred. Short bond length stretched of 0.005 A and 0.01 A of one of the $C-O$ bonds leads to large emphasis of the S-T structure.

The B3LYP wave function, with the cc-pVDZ basis set at the experimental geometry reveals a slight preference for the $S-T$ form. Increasing the basis set to cc-

pVTZ yields equal contributions of the $D-D$ and $S-T$ conformations. With the cc-pVDZ basis set and lengthening the $C-O$ bond reveals that the $S-T$ form is slightly preferred over the $D-D$ form. However, for the cc-pVDZ basis the same perturbations of the $C-O$ bond length reveal a preference for the $D-D$ configurations over the $S-T$ configuration.

CS_2^+ Analysis

For CS_2^+ the $^2\Pi_g$ and $^2\Pi_u$ adiabatic surfaces are separated by 20,975 cm^{-1} compared to 27,300 cm^{-1} [2, 6] for CO_2^+. Because the CS_2^+ surfaces of are not as widely separated as those for CO_2^+, vibrational and state mixing are expected to be more important than for CO_2^+**,** leading to a lower value of the asymmetric stretch frequency, ω_3 and a preference for the $S-T$ configuration. However, the charge distributions of the C and S atoms in CS_2^+ are closer in value to each other than are those for C and O in CO_2^+; leading to the expectation that $S-T$ configuration should be less dominant.

ELF analysis reveals that there are 9 attraction basins in the system, similar to CO_2^+: 3 core basins $C(C), C(S_1)$ and $C(S_2)$ one valence basin located between the C and S atoms, $V(C,S_1)$ and $V(C,S_2)$ two valence basins located on each of the S atoms: $V(S_1)$ and $V(S_2)$. The projections of the basin populations for UHF, MP2, and B3LYP-DFT wave functions with the cc-pVDZ and cc-pVTZ basis sets, are computed at the experimental geometry, and small distances slightly extended by 0.005 A and 0.01 A

along one of the $C-S$ bonds. The contribution results for UHF, MP2, and B3LYP-DFT wave functions for both cc-pVDZ and cc-pVTZ basis sets are given in Table 4.

The results of the UHF wave function at the experimental geometry of 1.564 A determine that the $S-T$ configuration is slightly preferred with the cc-pvDZ and cc-pvTZ basis sets. Lengthening one of the $C-S$ bonds give a small preference of the $D-D$ configuration.

The results of the MP2 wave function at the experimental geometry determine that the D-D form is slightly favored using the cc-pVDZ basis set, however this preference is lost with the cc-pVTZ basis set. Lengthening one of the $C-S$ bonds reveals a preference for the $D-D$ configuration regardless of the basis set used.

The results of the B3LYP-DFT wave function at the experimental geometry determine that the $S-T$ configuration is slightly preferred regardless of the basis set. Perturbation of one of the $C-S$ bond lengths reveals the dominance of the D-D configuration for both the cc-pVDZ and cc-pVTZ basis sets.

Conclusions

A CASSCF TF is found to give a DMC atomization energy of CO_2^+ of 226(1.8) kcal/mol which is in excellent agreement with the experimental value of of 225.3 kcal/mol. The DMC heat of formation at 298K was computed to be 382(1.8) is also in excellent accord with the experimental value 381 kcal/mol. We note that the B3LYP-DFT value of the atomization energy at the complete basis limit lies within 1.7 kcal/mol of experiment and the heat of formation is within 3.23 kcal/mol of experiment for the subject system. The

CCSD(T) results for the infinite basis set extrapolation are within experimental error, however the estimated heat of formation is 2.3 kcal/mol larger than experiment.

Through ELF analysis the quantitative contributions of the resonance forms to the ground state geometry of CO_2^+ and CS_2^+ at the UHF, MP2 and B3YLP-DFT levels of theory have been determined. We are able to directly quantify that for CO_2^+ the UHF and MP2 methods the $S-T$ structure is preferred for both the ground state geometry with $D_{\infty h}$ symmetry and perturbed geometries. The UHF asymmetric stretching frequency is computed to lie 464 cm^{-1} lower than experimental value of 1423 cm^{-1} [29]. Including electron correlation at the MP2 level of theory results in an imaginary value of the asymmetric stretch frequency. The B3LYP-DFT method successfully determines the $D-D$ structure to be preferred in the ground state of CO_2^+. The value of the asymmetric stretching frequency calculated at the B3LYP-DFT level of theory compares well to experimental results. In is in part due to that the $D-D$ structure is preferred. ELF calculations of the CS_2^+ demonstrate that UHF, MP2, and B3LYP wave functions predict the $D-D$ resonance form to be preferred. As a result, the asymmetric stretch is fairly well predicted by the three methods compared to experiment [30, 31]

VI Acknowledgments

The authors were supported by the Director, Office of Science, Office of Basic Energy Sciences, Chemical Sciences Division of the U. S. Department of Energy under Contract No. DE-AC03-76SF00098.

References

[1] M.A. Johnson and J. Rostas, Mol. Phys. 839 (1995) 85.

[2] G. Herzberg, Molecular Spectra and Molecular Structure III: Electronic Spectra and Electronic Structure of Polyatomic Molecules, D. Van Nostrand Company, Inc., New York, 1966.

[3] G.I. Gellene, J. Chem. Phys. 15393 (1996) 100.

[4] G.I. Gellene, Chem. Phys. Lett. 315 (1998) 287.

[5] S. Carter, N.C. Handy, P. Rosmus, and G. Chambaud, Mol. Phys. 605 (1990) 71.

[6] J.M. Frye and T.J. Sears, Mol. Phys. 919 (1987) 62.

[7] B.L. Hammond, W.A. Lester, Jr., and P.J. Reynolds, Monte Carlo Methods in Ab Initio Quantum Chemistry. World Scientific Lecture and Course Notes in Chemistry. Vol. 1, World Scientific, Singapore, 1994.

[8] K.E. Schmidt and J.W. Moskowitz, J. Chem. Phys. 4172 (1990) 93.

[9] S.F. Boys and N.C. Handy, Proc. R. Soc. London Ser. A. 43 (1969) 310.

[10] R.J. Jastrow, Physica. 1161 (1956) 22.

[11] R.J. Jastrow, Phys. Rev. 1484 (1955) 98.

[12] A. Aspuru-Guzik, O. Couronne, I. Ovcharenko, and W.A. Lester, Jr., *Deviation minimization for quantum Monte Carlo wavefunction optimizaion*. 2002.

[13] M. Krauss and W.J. Stevens, Ann. Rew. Phys. Chem. 357 (1984) 35.

[14] W.J. Stevens, H. Basch, and M. Krauss, J. Chem. Phys. 6026 (1984) 81.

[15] T.H. Dunning, J. Chem. Phys. 1007 (1989) 90.

[16] M.S. Gordon, M.W. Schmidt, G.M. Chaban, K.R. Glaesemann, W.J. Stevens, and C. Gonzalez, J. Chem. Phys. 4199 (1999) 110.

[17] A.D. Becke, J. Chem. Phys. 5648 (1993) 98.

[18] J.A.W. Harkless and W.A. Lester, Jr., J. Chem. Phys. 2680 (2000) 113.

[19] P.J. Linstrom and W.G. Mallard, eds. *NIST Chemistry WebBook, NIST Standard Reference Database Number 69,*. 2001, July 2001, National Institute of Standards and Technology: Gaithersburg, MD.

[20] M.W. Chase, ed. *JANAF Thermochemical Tables*. 3 ed. Vol. 1-2. 1986, American Chemical Society: Washington.

[21] A.D. Becke and K.E. Edgecombe, J. Chem. Phys. 5397 (1990) 92.

[22] X. Krokidis, S. Noury, and B. Silvi, J. Phys. Chem. A. 7277 (1997) 101.

[23] B. Silvi, Nature. 683 (1994) 371.

[24] X. Krokidis, V. Goncalves, and A. Savin, J. Phys. Chem. A. 5065 (1998) 102.

[25] X. Krokidis, N.W. Moriarty, W.A. Lester, Jr., and M. Frenklach, Chem. Phys. Lett. 534 (1999) 314.

[26] S. Noury, X. Krokidis, F. Fuster, and B. Silvi, Comp. Chem. 597 (1999) 23.

[27] M.J. Frisch, G.W. Trucks, H.B. Schlegel, G.E. Scuseria, M.A. Robb, J.R. Cheeseman, V.G. Zakrzewski, J.A. Montgomery, R.E. Stratmann, J.C. Burant, S. Dapprich, J.M. Millam, A.D. Daniels, K.N. Kudin, M.C. Strain, O. Farkas, J. Tomasi, V. Barone, M. Cossi, R. Cammi, B. Mennucci, C. Pomelli, C. Adamo, S. Clifford, J. Ochterski, G.A. Petersson, P.Y. Ayala, Q. Cui, K. Morokuma, D.K. Malick, A.D. Rabuck, K. Raghavachari, J.B. Foresman, J. Cioslowski, J.V. Ortiz, B.B. Stefanov, G. Liu, A. Liashenko, P. Piskorz, I. Komaromi, R. Gomperts, R.L. Martin, D.J. Fox, T. Keith, M.A. Al-Laham, C.Y. Peng, A. Nanayakkara, C. Gonzalez, M. Challacombe, P.M.W. Gill, B.G. Johnson, W. Chen, M.W. Wong, J.L. Andres, M. Head-Gordon, E.S. Replogle, and J.A. Pople, *Guassian 98*. 1998, Gaussian Inc.: Pittsburg.

[28] M.W. Schmidt, K.K. Baldridge, J.A. Boatz, S.T. Elbert, M.S. Gordon, J.H. Jensen, S. Koseki, N. Matsunaga, K.A. Nguyen, S. Su, T.L. Windus, M. Dupuis, and J.A.J. Montgomery, J. Comp. Chem. 1347 (1993) 14.

[29] K. Kawaguchi, C. Yamada, and E. Hirota, J. Chem. Phys. 1174 (1995) 82.

[30] W.J. Balfour, Can. J. Phys. 1969 (1976) 54.

[31] L.S. Wang, J.E. Reutt, Y.T. Lee, and D.A. Shirley, J. Electron. Spectrosc. 167 (1988) 47.

Table 1: Natural orbital occupation numbers for MP2 and CASSCF wave functions

	NO Occupation	
Orbital	MP2	CASSCF[a]
1	2.06184	1.99754
2	2.00001	1.98001
3	2.00001	1.99001
41	-0.00062	0.00002
42	-0.06230	0.00002

[a]CASSCF wavefunction in which 7 electrons have been distributed amongst 8 orbitals

Table 2: Ab initio atomization energies and heats of formation[a]

Method	E_a (kcal/mol)	ΔH_f^{298} (kcal/mol)
ROHF	228.8	379.7
MP2	3961.	212.7
LDA	455.9	152.9
B3LYP	379.3	229.5
CCSD(T)	380.3	228.5
DMC		
HF[b]	374.0(1.2)	234.4(1.2)
NO[c]	382.1(1.8)	226.6(1.6)
Expr.	381	225.3

[a]ROHF, MP2, LDA, B3LYP, and CCSD(T) are results of extrapolations to the complete basis set limit.

[b]DMC trial wave function using orbitals obtained from HF

[c]DMC single determinant trial wave function using NOs obtained from CASS(7,8)

Table 3: Single-Triple (S-T) and double-double (D-D) contributions to the ground state and two perturbed geometries of CO_2^{+} [a].

Method	Basis Sets/contributions of resonance structures													
	cc-pVDZ							cc-pVTZ						
	[b]		[c]		[d]			[b]		[c]		[d]		
	S-T	D-D	S-T	D-D	S-T	D-D	ω_3 [e]	S-T	D-D	S-T	D-D	S-T	D-D	ω_3 [e]
UHF	0.482	0.512	0.402	0.592	-	-	959	0.495	0.485	0.465	0.515	0.347	0.647	829
MP2	0.487	0.507	0.407	0.587	0.387	0.607	1674i	0.495	0.485	0.475	0.505	0.357	0.637	1795i
B3LYP	0.512	0.482	0.472	0.522	0.452	0.654	1495	0.497	0.497	0.482	0.528	0.477	0.517	1472

[a]The $C\text{-}O_1$ bond length is fixed at 1.177 A for all geometries. S-T is the single-triplet and D-D is the double-double bonded resonance forms (see figure 1).

[b]$C\text{-}O_2$ = 1.177 A

[c]$C\text{-}O_2$ = 1.182 A

[d]$C\text{-}O_2$ = 1.187 A ELF calculation failed to converge for the UHF wave function.

[e]Asymmetric stretch (cm^{-1}). Vibrational frequencies listed above are unscaled Experimental value of the asymmetric stretch is 1423 cm^{-1} [29].

Table 4: Single-triple (S-T) and double-double (D-D) contributions to the ground state and two perturbed geometries of CS_2^{+} [a].

Method	Basis Sets/contributions of resonance structures													
	cc-pVDZ							cc-pVTZ						
	[b]		[c]		[d]			[b]		[c]		[d]		
	S-T	D-D	S-T	D-D	S-T	D-D	ω_3 [e]	S-T	D-D	S-T	D-D	S-T	D-D	ω_3 [e]
UHF	0.508	0.488	0.468	0.528	0.463	0.533	1182	0.503	0.493	0.473	0.523	0.463	0.533	1216
MP2	0.503	0.493	0.473	0.523	0.468	0.528	1058	0.493	0.503	0.468	0.528	0.468	0.528	1225
B3LYP	0.508	0.488	0.463	0.533	0.463	0.528	1236	0.503	0.493	0.483	0.513	0.478	0.518	1239

[a]The C-S_1 bond length is fixed at 1.564 A for all three geometries. S-T and D-D are the single-triple and double-double bonded resonance form respectively (see figure 2)

[b]C-S_2 = 1.564 A

[c]C-S_2 = 1.569 A

[d]C-S_2 = 1.574 A

[e]Asymmetric stretch (cm^{-1}). Vibrational frequencies listed above are unscaled Experimental value of the asymmetric stretch is 1203 cm^{-1} [30, 31].

FIGURE CATIONS

Figure 1 Single-triple (S-T) and double-double (D-D) resonance forms of CO_2^+.

Figure 2 Single-triple (S-T) and double-double (D-D) resonance forms of CS_2^+.

Figure 3 Electron localization function (ELF) calculated for CO_2^+. There are 9 basins of attraction in the system: 3 core basins $C(C)$ labeled, $C(O_1)$ and $C(O_2)$, two valence basins located between the carbon and oxygen atoms labeled here as $V(C,O_1)$ and $V(C,O_2)$, and two valence basins located on each of the oxygen atoms: labeled, $V(O_1)$ and $V(O_2)$.

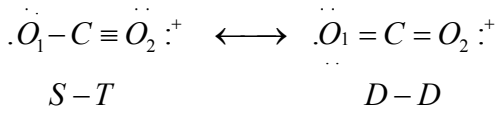

Figure 1

$$\underset{S-T}{.\dot{S}_1 - C \equiv \dot{S}_2 :^{+}} \quad \longleftrightarrow \quad \underset{D-D}{.\dot{S}_1 = C = S_2 :^{+}}$$

Figure 2

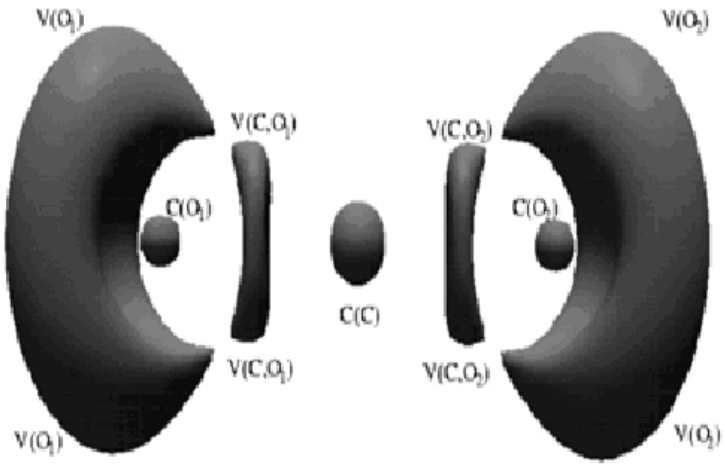

Figure 3